

NEW LARGE GEOTHERMAL STORAGE PROJECT IN ZÜRICH/SWITZERLAND FOR HEATING AND COOLING

E. Rohner, T. Kohl, Geowatt AG, Dohlenweg 28, CH-8050 Zürich, Switzerland

Abstract: During the renovation of a major Grand Hotel in Zurich a complete new domestic heating and cooling system was installed. A gas-driven absorption heat pump will supply the required heating and cooling energy. A massive reduction of electricity costs in summer is intended. A geothermal energy storage of $\sim 250'000 \text{ m}^3$ will be exploited by borehole heat exchangers with totally $\sim 10'000 \text{ m}$ length. Supported by additional heat recovery, the subsurface storage will supply 1 GWh in winter. From spring to autumn, the hotel will be cooled (1 GWh) by the same storage system. Additional waste heat will be used for hot water generation. The paper describes the effects of different utilization concepts to the thermal subsurface fields. In particular, the requirements of a hotel specializing in wellness spa applications involve sophisticated dimensioning of this low-enthalpy plant. The 3D model accounts for individual thermal interaction of the borehole heat exchangers in surface and for different topographic and climatic conditions at this mountainous site.

Key Words: *Heat pump, geothermal energy storage, heating and cooling*

1 INTRODUCTION

During its renovation and extension the Grand Hotel Dolder (The Dolder Grand) will be equipped by a complete new heating and cooling system required for the hotel operation and the planned activity for wellness relaxing of the hotel guests. It was intended that heating and cooling operation be mainly covered by a geothermal storage system.

The kernel of the planned installations is a gas driven absorption heat pump used for both heating and cooling tasks. The main reasons are a massive reduction of electric energy in summer month for the cooling operation. In winter, the geothermal energy storage shall be discharged and increased to operational heating and warm water supply temperature by the absorption heat pump. The heat pump is supported by a domestic wastewater heat recovery, with the waste water being conducted for reheating over a special plate heat exchanger. Starting in spring the hotel will be cooled through the geothermal energy storage until beginning autumn. The hot water generation is carried out again by the absorption heat pump. The required cooling power supports the cooling of the building. In addition water coolers are available for cooling (especially for dehumidification).

A total volume of $200'000 \text{ m}^3$ is available in the ground for the geothermal energy storage. A first rough calculation has lead to a planning of 81 borehole heat exchangers, each with 127 m length on a 5 m x 5 m pattern to cover the required heating and cooling needs.

For further optimizing the storage, detailed three-dimensional simulations have been conducted that will be presented in the present manuscript.

The investigations have been conducted to achieve the following goals:

1. correct and optimum dimensioning of the geothermal storage with high efficiency and cost control. Especially, minimizing depth and number of borehole heat exchangers.
2. Influence of an insulation of pipes and or conduits to the efficiency of overall system.

2 NUMERICAL SIMULATIONS

2.1 Background

For the simulation of the thermal behavior of a borehole heat exchanger (BHE) a finite element (FE) simulator has been developed that is based upon the well-experienced FE code FRACTure (Kohl and Hopkirk, 1995). FRACTure offers complete three-dimensional solutions of steady-state or transient hydraulic, thermal or elastic processes. Each process can be simulated by 1D-, 2D- or 3D element types. Each of them can have linear or quadratic shape functions. The simulations assume the following thermal transport mechanisms: transient change of energy content, diffusion, advection and heat transfer. These mechanisms are described by the following equations (Kohl and Hopkirk, 1995):

$$\overline{\rho c_p} \cdot \frac{\partial T}{\partial t} = \nabla \cdot (\bar{\lambda} \cdot \nabla T) - [\rho c_f]_f \cdot v \cdot \nabla T + h \cdot \frac{A}{V} \cdot \Delta T$$

with T temperature, t time [s], $\overline{\rho c_p}$ thermal capacity of the porous medium or of the fluid [J/m³/K], $\bar{\lambda}$ thermal conductivity of porous soil or fluid [W/m/K], v Darcy-flow velocity [m/s], ρc_f heat capacity of fluid [J/m³/K], h heat transfer coefficient [W/m²/K], A cross-sectional area at heat transfer [m²] and V volume [m³].

The FE-scheme allows a flexible structure of the discretized mesh and, therefore, can adopt complex geological or technical geometries (like the construction with heat transfer across the pipe wall of a BHE).

2.2 Model geometry

As first simplification of the problem posed, the boundary conditions are placed at the distance that a mutual influence of BHE does not occur, or that they match a symmetry condition. The latter-one is used to match the heat exchange between BHE on the selected 5 m x 5 m pattern. Since the minimum depth of the model had to match the length of the BHE, much deeper grids were established, with a single BHE in the center of a cell. According to these considerations only a single BHE has been simulated adopting symmetry boundary conditions and neglecting edge or border effects at the storage volume. During construction, the conduits are placed in 20 cm thick gravel concrete under the 70 cm thick bottom plate. In order to have a minimum influence between the conduits, an orthogonal pattern of the feed and return pipes is established. A 15 cm thick insulation layer runs between bottom plate and gravel concrete. Since all BHE are placed below the building, this insulation offers the advantage that the heat load of the building is not transferred in the realm of the BHE and of the conduits. All specified materials have been treated in the numerical model.

In the near-field around the BHE a fine discretization of the mesh is required to resolve for the complex temperature behavior. Individual nodes have a millimeter to centimeter distance to each other. The number of nodes can be quickly roughened to lower the CPU computing requirements. In vertical direction, the model is extended until 500 m, to reduce possible boundary effects. The lateral areas of the model are assumed to be "tight", i.e. no heat exchange can take place (symmetry, Neuman-type boundary condition).

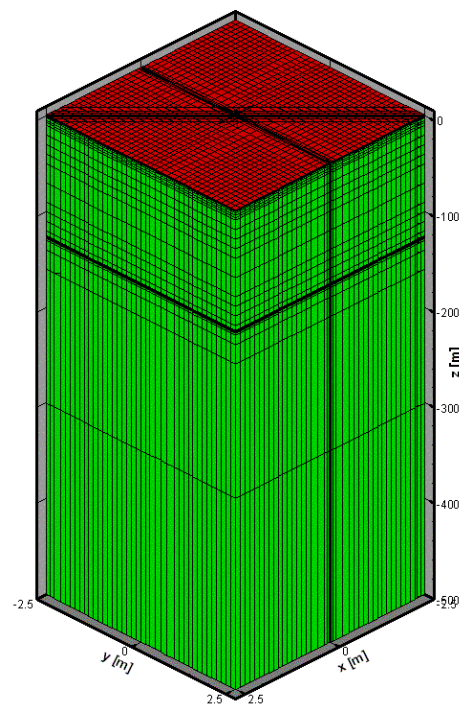


Figure 1: 3D-Model. The discretization of the orthogonal and diagonal conduits is well visible.

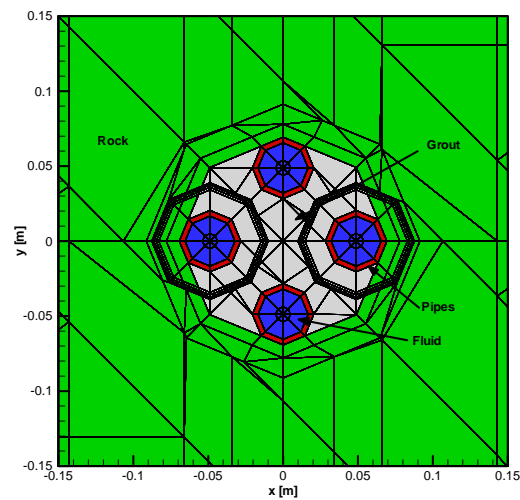


Figure 2: 2D-section of BHE, the discretization permits for an insulation of the return pipes.

2.3 Material sets

Table 1: Used material parameters

Material	Thermal Conductivity [W/m/K]	Heat capacity [MJ/m ³ /K]
Rock	2.30	2.40
Pipes	0.42	1.42
Grout	0.80	2.00
Fluid	0.60	4.18
Foundation	1.80	2.64
Isolation	0.04	0.05

2.4 Boundary conditions

The temperature profile determined by a temperature log at undisturbed subsurface on April 30th, 2004, is assumed to be the initial condition for the model. Since all BHE are placed below the building, the temperature will not be determined by climatic or weather influences but by the calculated heat exchange between building and soil. A constant heat flow condition of 5 W/m² is therefore assumed at the model surface. At the base of the model a geothermal heat flow of 0.09 W/m² is simulated.

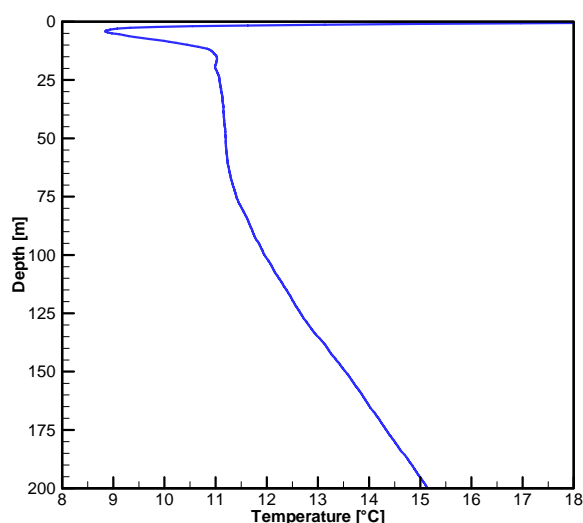


Figure 3: Initial temperature profile

The BHE operation (Injection and extraction of heat) is simulated according to the energy balance of the building and of the working temperature of the heat pump. In winter operation (Months with negative energy balance, see Table 2) the absorption heat pump works with fixed return temperature RLT (in relation to the BHE) of 11°C and results in a fixed supply temperature (VLT) of 7°C. If the 11°C cannot be realized by the BHE field, the heat pump is additionally supplied by the heat recovery device. During summer operation (months with positive energy balance; Table 2) the commercial and cooling plants require a RLT of 14°C and provide a VLT of 19-21°C. If the 14°C cannot be realized by the BHE field, external refrigerating machine start operation. In our notation, T_{in} represents the real entry temperature in the BHE, and T_{out} corresponds to the temperature required to cover the planned energy balance. If T_{out} cannot be reached by the BHE field, heat recovery or refrigerating machines start operation.

Table 2: Energy balance, supply (T_{in}) and return temperature (T_{out}) in relation to BHE.

	Heat supply [MWh]	Cool supply [MWh]	Balance [MWh]	T_{in} [°C]	T_{out} [°C]	ΔT [K]
January	187	38	-149	7	11	-4
February	161	41	-120	7	11	-4
March	120	58	-62	7	11	-4
April	89	109	20	19	14	5
May	67	129	62	19	14	5
June	49	155	106	20	14	6
July	49	192	143	21	14	7
August	53	175	122	21	14	7
September	80	109	29	20	14	6
October	107	67	-40	7	11	-4
November	137	41	-96	7	11	-4
December	151	38	-113	7	11	-4

The energy balance and the "desired" exit temperature of the BHE determine the nominal flow velocity v_{BHE} [m/s] along the BHE according to the following relation:

$$v_{BHE} = \frac{q}{A_{BHE}} = \frac{P}{A_{BHE} \cdot \rho c_p \cdot \Delta T}$$

with q flow rate [m³/s], A_{BHE} cross-sectional area of the pipes [m²], P thermal power [W] and ρc_p heat capacity of the fluid [J/m³/K].

The monthly varying flow rates are fully calculated in the FE scheme by applying individual load-time functions.

In comparison to a usual BHE plant with a ΔT of 3 K, the actual system operates especially in summer with much higher differences between entry and exit temperatures, whose influence is - among others - subject to the following detailed analysis.

3 RESULTS

3.1 BHE numbers

The first investigation focused on the influence of a lower number of BHE to the exit temperature. The system has been simulated for a whole annual operation cycle. The calculations have investigated a standard dimensioning (81 BHE each with 127 m depth) and two additional test cases with 70 and 60 BHE. Figure 4 represents the temperature history at BHE exit for each case. Concerning the required temperature of 11°C ($T_{in} = 7^\circ\text{C}$) it was concluded at that stage that the BHE field could cover in average roughly 50% of the energy balance during winter operation (Figure 5). The heat recovery device should deliver the remaining 50%. In summer time, the total energy need is only fully covered in April and May by "Free-Cooling". In average more than 70% of the total energy is produced by the BHE field. During extreme hot summer days, an activation of the water-coolers can become necessary.

The exit temperatures deteriorate by 0. K in winter and in summer by 0.3°C using 70 instead of 81 BHE (each at 127 m depth). With 60 BHE the difference would be more than 0.5 K.

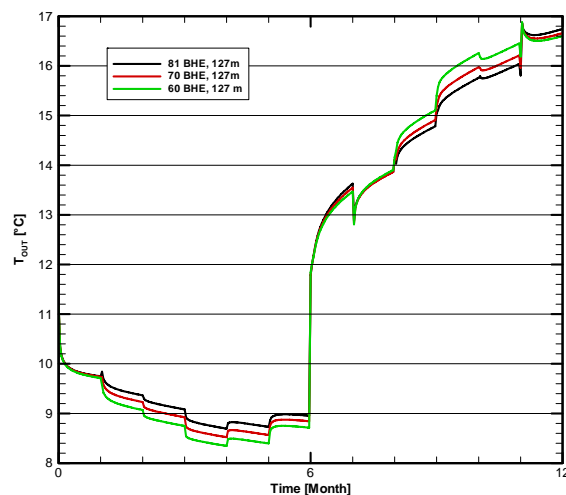


Figure 4: Comparison of T_{out} history in first operation year with 81, 70 or 60 BHE, each with 127 m depth.

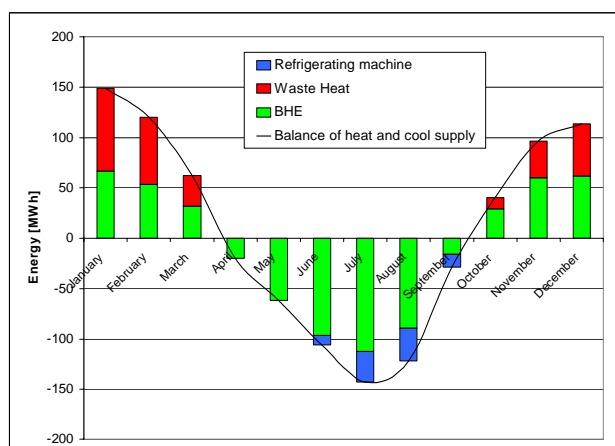


Figure 5: Energie balance for standard case (81 BHE, each with 127 m depth)

3.2. Vertical insulation of BHE pipes

Due to the high difference between entry and exit temperature in the BHE (see Table 2), a relative large thermal interaction between supply and return pipes can develop. Figure 6 illustrates the temperature profile along the BHE in December and July. It was concluded that the warmer supply pipes would heat the return pipes by more than 1.5 K!!!

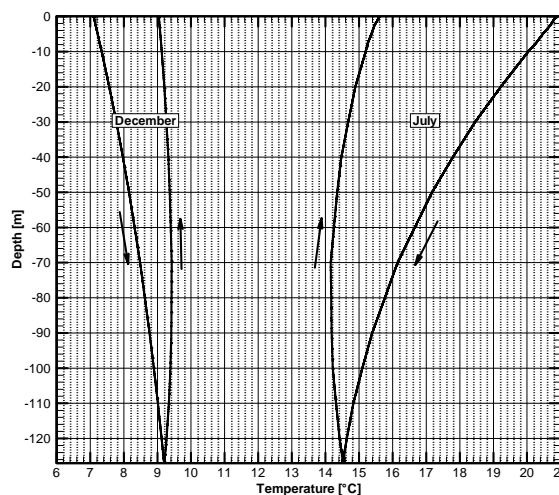


Figure 6: Vertical temperature profile along the BHE in December and July, when not insulating the BHE pipes. The arrows illustrate the flow direction

A vertical insulation of the BHE return pipes is therefore simulated. In agreement to practical construction, an insulation of the topmost 20 m of the BHE return pipes are simulated. In addition, also an insulation until 50 and 70 m depth is calculated for comparison. Figure 8 represents the results.

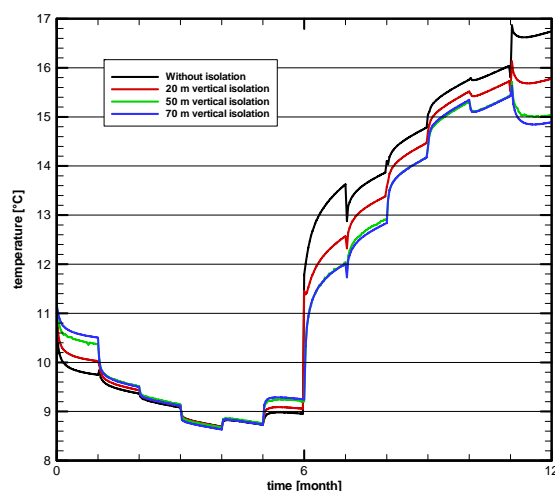


Figure 7: Comparison of T_{out} history in first year of operation applying different insulations of the topmost 20, 50 and 70 m of the BHE return pipe.

It has been demonstrated that especially in summer, an insulation of the return pipe has a high potential for improvement. At a 20 m deep insulation, until 0.5 K lower exit temperatures can result. With 50 m insulation, even 1 K lower exit temperature would rise; deeper insulation doesn't show any improvement. Figure 8 illustrates the vertical temperature profile along BHE for the different test cases at end of July.

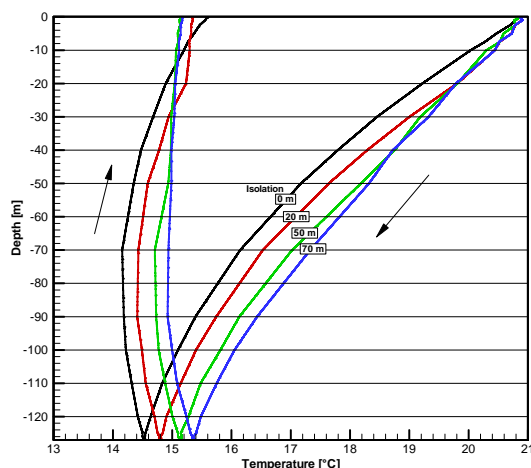


Figure 8: Temperature profile along BHE, End of July of the first operation year, with and without insulating the topmost 20, 50 and 70 m of the return pipes. The arrows illustrate the flow direction.

However, also insulation can have a disadvantage. The heat that cannot be transferred to the return pipes will yield an increase of the temperature of the supply pipes.

3 CONCLUSIONS

There is still a lack of experience in dimensioning complex heating / cooling systems. The presented examples illustrate, what optimizing potential the geothermal storage systems have. Conventional dimensioning tools are here only of little use, since they oversimplify especially the cooling cycle during summer. Our calculations have demonstrated on the example of insulating the return pipe of a BHE which thermal interactions can occur. In future, the combined heating/cooling of buildings by geothermal storage systems will certainly be more popular. The renovation and extension of The Dolder Grand in Zurich is an innovative example of the continuous engineering.

ACKNOWLEDGEMENTS

The authors would like to thank Markus Geissmann from the Federal Office of Energy of Switzerland for supporting the planning and control of this otherwise fully privately financed project.

REFERENCES

Kohl T., R.J. Hopkirk 1995: "'FRACTure" a simulation code for forced fluid flow and transport in fractured porous rock", *Geothermics*, 24(3), pp. 345-359